

Low-Discrepancy Distribution of Points on Arbitrary Polygonal 3D-surfaces

Alena Bulyha, Wolfgang Herzner, Markus Murschitz and Oliver Zendel
Safety & Security Department, AIT Austrian Institute of Sciences,
Donau-City-Straße 1, 1220 Vienna, Austria

Keywords: 3D-surfaces, Geometric Discrepancy, Halton Sequences, Hammersley Sequences, Low-Discrepancy, Sampling, Segmentation, Uniform Distribution, Unfolding, Wrapping.

Abstract: This paper presents a technique for automatic distribution of points on 3D-surfaces that are defined as meshes of polygons (usually triangles) such that the distribution has a low discrepancy. The work is motivated by the quest for representing arbitrary 3D-objects by a minimal number of surface points such that different views and arbitrary occlusions of objects can be effectively distinguished by simply using the visible surface points. The approach exploits low-discrepancy sequences on the unit square such as those proposed by Hammersley or Halton.

1 INTRODUCTION

In computer graphics, a standard technique for modelling the geometry of 3D-objects is to represent their surface as polygon meshes, mostly consisting of triangles. The question we want to address in this work is: how to distribute points on a polygonal mesh of a 3D-object such that for each possible view (2D-projection) of the object, the visible fraction of points can be used as representative for the visible fraction of its total surface in that view? Of course, for economic reasons the question should be extended by “with as few points as possible”.

A hint for a possible answer can be found in 2D-geometry. Consider you want to distribute a set P of n points on a square U such that for any sub-area $R \subseteq U$, larger than some given minimum, the ratio of points contained in R to n is as close as possible to the ratio of the areas of R and U ; i.e. the number of points found in R can be used as a good approximation for the size of R relative to U . It turns out that both regular and random distributions are not well suited for that purpose, while in the case of continuous uniform distributions, the local point density is proportional to the surface area covered by these points. This is illustrated in Figure 1.

The measure for the deviation between the real size and that indicated by the number of covered points is called geometric discrepancy (see chapter 2

for precise definitions and more background). Evidently, the smaller this value the better.

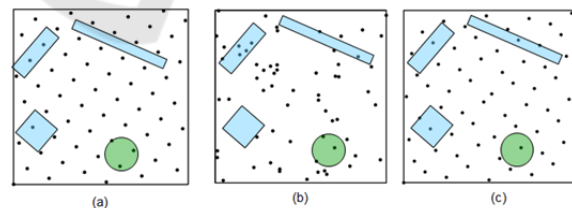


Figure 1: Point distribution examples on a square: (a) the points arranged in a lattice; (b) random (Monte Carlo) points; (c) Hammersley points.

Actually, low-discrepancy point sets have been widely used in computer graphics and image processing for point based object representation (Quinn et al., 2007), for improving image quality (Wong et al., 1997), for the purpose of antialiasing (Wand and Straßer, 2003), for half-toning (Hanson, 2003) or for illumination (Dachsbacher and Stamminger, 2006).

Several methods for producing low-discrepancy sequences on the unit square have been proposed by Hammersley (Hammersley, 1960), Halton (Halton, 1960), Sobol (Sobol, 1967), Niederreiter (Niederreiter and Chao, 1995) and have been further investigated by other scientists or research groups (Cheng and Druzdzel, 2000, Grabner et al., 2012).

This work addresses uniform distribution of points on arbitrary polygonal 3D-surfaces. The idea

is to unfold the polygon resulting in a 2D- representation, then to place low-discrepancy distributed points on it, and finally, to map these placements back to the 3D object. The discrepancy is treated in this work only analytically. To control the quality of the performed technique, the irregularity measure as a comprehensible geometric interpretation is presented and is explained by the algorithm and several examples. The proposed approach concentrates only on triangular meshes. However, the method could also be extended for surfaces represented by arbitrary polygons.

This paper is structured as follows. In the next section, similar work found in literature is shortly discussed, while Section 3 introduces the mathematical background of geometric discrepancy. Section 4 describes our method and its evaluation criteria. Section 5 presents and discusses some application examples and Section 6 draws a conclusion.

2 RELATED WORK

Previous research in the area of sampling techniques mainly concentrated on uniform scattering of points on planar domains (Pillardts and Cools, 2005, Hofer and Pirsic, 2011) and on spherical surfaces (Rakmanov et al., 1994, Cui and Freeden, 1997).

More recent investigations address low-discrepancy point distributions on an arbitrary surface. They include different sampling strategies based on uniform distribution of lines in the 3D space, on space filling curves. For instance, Quinn (Quinn et al., 2007) use Hilbert curves to fill parameterized meshes and map them onto the surface. The low-discrepancy sampling happens along the Hilbert curves. The parameterization methods are based on solving the sparse linear system and can be applied only to surface-sections that are homeomorphic to a disk. Thus, the pre-processing step is also applied to cut an arbitrary mesh into a set of topological disks and to generate the Hilbert curves. Because the choices of parameterization and cutting algorithms have little effect on the final sampling due to the adaptive nature of the Hilbert curve and the remeshed surface of the object can be slightly changed during this process, the Hausdorff distance is used to assess how well the new shape is preserved. Our approach, however, is shape accurate and is easy to implement. The initial mesh is not changed when providing the low-discrepancy distribution over the planar domain and mapping it back to the original surface.

Rovira (Rovira et al., 2005) suggest a sampling technique based on intersecting of lines uniformly distributed in 3D-space with polygonal models. Several algorithms to generate the set of uniformly distributed lines are proposed. Each of them utilizes the low-discrepancy point set in four dimensions and is based on the approximation of a binomial distribution by a Poisson distribution. Such approximation is only suitable for large number of lines. Thus, the proposed approach causes the large number of uniformly distributed lines and, therefore, the large number of intersecting points. In contrast, using the scattering of the 2D low-discrepancy points set onto the surface our algorithm can deal with a small number of sampling points.

Our approach is also related to prior works on mesh segmentation and mapping the segments onto a planar domain (also called mesh unwrapping or unfolding). The partitioning techniques of boundary meshes is often application dependent. In fact, it can be distinguished between two general types: segmentation of the whole object into meaningful, volumetric parts and partitioning of the surface mesh into segments under some criteria. A detailed overview of these methods is given in (Shamir, 2008). The work described in this paper does not concern optimal segmentation, but a simple unfolding algorithm has been designed to fulfil the given goals.

3 MATHEMATICAL BACKGROUNDS

Let P be a set of n_U points that are distributed on the unit square $U=[0,1)\times[0,1)$.

Collection S_2 is the set of *sampling figures* on the unit square U . In general, it can be any set consisting of scaled and translated copies of fixed polygons or polytopes (Matousek, 1999 p.10). Therefore, S_2 can include such sample figures F which contain the unit square or some part of it or do not overlap with U . As only overlap with U is of interest, the collection shall be reduced to the set $\{R \mid R=F\cap U\}$. Without any further notation, let R be an element from collection S_2 and $R \subseteq U$.

$N(R)$ is the number of points of P within R and, therefore, $N(U)=n_U$. The *geometric discrepancy* D for the unit square U can be defined (Matousek, 1999, p.13, Alexander, 2004, p.283) by taking a norm of the difference between the actual number of points within any sampling figure R and the expected number of points hitting R , i.e.

$$D(U, P, S_2, L) := \|n_U \text{vol}(R) - N(R)\|_L, \quad (1)$$

where $R \in S_2$. $vol(R)$ denotes the area of R , as fraction of U , i.e. $vol(R) := area(R)/area(U)$, and $n_U vol(R)$ is the expected number of points hitting R . The function $\Delta(R) = n_U vol(R) - N(R)$ is denoted as **discrepancy function** with the following norm:

$$\|\Delta(R)\|_L = \left(\int_{S_2} (\Delta(R))^L d\mu \right)^{1/L}, \quad 1 \leq L < \infty, \quad (2)$$

$$\|\Delta(R)\|_\infty = \sup_{R \in S_2} |\Delta(R)|, \quad (i.e. L = \infty); \quad (3)$$

Let $d_m := 1/\sqrt[n_U]{n_U}$ be the **mean distance** between closest neighbour points, where $n_U = \#P$ is the cardinality of P that is equal to the prescribed density.

In our work we use the Hammersley or Halton sequences to calculate the potentially infinite uniformly distributed sequence W on the unit square, and utilize the first n points to build the set P . These sequences are based on radical inversion and modifications of this inversion (Halton, 1960, Hammersley, 1960). The sequences are defined in an arbitrary number of dimensions. An implementation of them is described in (Wong et al., 1997).

For every natural number n , the discrepancy for both Hammersley or Halton sequences is bound, i.e. there is an absolute positive constant c such that $|D(U, P, S_r, \infty)| \leq c |\log(n)|$, where $S_2 \equiv S_r$ is a set of axis-parallel rectangles (Matousek, 1999, p.41). We can also say in this case that the discrepancy satisfies $D(U, P, S_r, \infty) = O(\log(n))$.

If $S_2 \equiv S_d$ is a set of two-dimensional disks of radius r , and $n = \#P$, then there are two absolute positive constants c_1 and c_2 (Alexander, 2004, theorem 13.3.6) that depend on the radius. The discrepancy can be estimated as follows:

$$\begin{aligned} c_1(r) n^{1/4} &< D(U, P, S_d, \infty) \\ &< c_2(r) n^{1/4} \sqrt{\log(n)} \end{aligned} \quad (4)$$

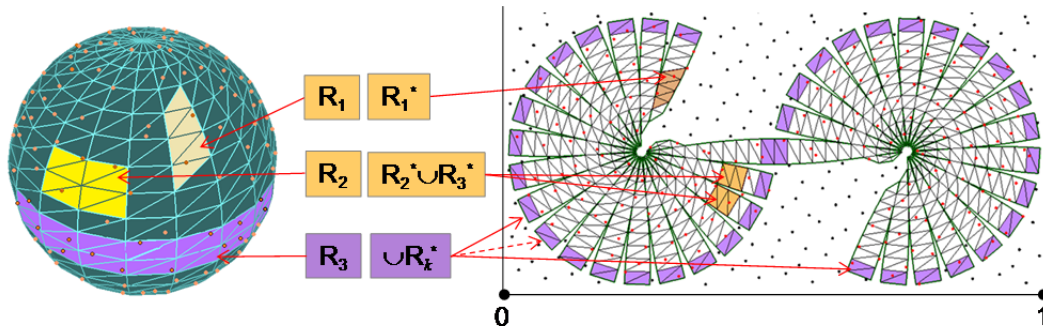


Figure 2: Example of the discrepancy calculation on the surface of a 3D-object.

Some further discrepancy estimations are also given in (Alexander, 2004, Berg, 1996, Chen and Travaglini, 2007).

Because the estimation of the discrepancy depends on the collection S_2 and used norm, we further assume that the collection is a set of different convex figures and is large enough; and the lower and upper bounds of discrepancy exist:

$$\underline{D}(\#P) \leq D(U, P, S_2, L) \leq \overline{D}(\#P). \quad (5)$$

As already mentioned in the introduction, we want to distribute points on 3D-surfaces by unfolding their meshes, mapping them to U , and remapping the “caught” points of P back to the surface.

If we apply only rotation, translation and isotropic scale for the mapping between planar surface elements and U , the transformed set of points is also uniformly distributed with only minor change in the discrepancy, see also concept of isotropic discrepancy in (Matousek, 1999).

To measure the discrepancy $D(O_M, Q, S_{OM}, L)$ of the points set Q on the surface of a 3D-object, a feasible collection S_{OM} of the sample figures should be selected. The collection proposed in (Quinn et al., 2007) is a sub-set of the triangulated object’s mesh (O_M or O_M) that is chosen as “a contiguous set of triangles, grown from a random seed triangle to a random number of triangle rings”. The mesh segments with random number of triangles could also be used instead of the ring of triangles.

As an example, consider some sphere with set of points $Q = \{q_{ij}\}$ scattered over its surface. The sphere is scaled in such a way that its unfolded mesh is measure-preserving mapped to the unit square, as is shown in Figure 2, where the mapped points $Q = \{q_{ij}\} \in O_M$ and the initial points $Q^* = \{q_i^*\} \in U$ are given in red colour.

The part of the unit square, which is not covered by the unfolded mesh, is completed with points $Q' = \{q'_{ij}\}$, i.e. $P^* = Q' \cup Q^*$, $P^* \in U$. The points Q' are shown in Figure 2 in black colour.

Let $S_{OM}^* = \{R_i^*\}$ be the set of the unfolded sample figures. For instance, in the given example the sample figure R_1 is unfolded to R_1^* , the figure R_2 is unfolded to convex figures R_2^* and R_3^* and the unfolded figure R_3 is the set of triangles pairs R_k^* .

Assume also that the set S_{OM}^* is reasonably extended to S_2^* and used to measure the discrepancy of P^* in the unit square, i.e. $S_{OM}^* \subset S_2^*$ and $\overline{D_U}(\#P^*) \leq D(U, P^*, S_2^*, L) \leq \overline{D_U}(\#P^*)$. Thus, each discrepancy function calculated in the unit square has an upper bound $\Delta(R_i^*) \leq \overline{D_U}(\#P^*)$, $\forall R_i^* \in S_2^*$.

Consider the discrepancy function calculated for the set of points on the spherical surface. Because isotropic mapping is used, the expected number of points and the real one inside the sample figure will not change after unfolding and, therefore, the discrepancy function of R_1 is $\Delta(R_1) = \Delta(R_1^*)$, where $R_1 \in S_{OM}$ and $R_1^* \in S_2^*$. For the sample figure $R_1 \in S_{OM}$ the discrepancy function is calculated as $\Delta(R_2) = \Delta(R_2^*) + \Delta(R_3^*)$.

The strongest influence on the discrepancy $D(O_M, Q, S_{OM}, L)$ is given by a sample figure like $R_3 \in S_{OM}$, i.e. $\Delta(R_3) = \sum_{k_3}^{f_3} \Delta(R_{k_3}^*)$, $f_3 = 39$. The influence of the sample figures $R_{k_i}^*$ on the discrepancy decreases with increased density of distributed points, i.e. with increase of the cardinality of Q . For each $R_{k_i}^*$ there exists an absolute positive constant $c_{k_i}(\#Q) \leq 1$, such that each discrepancy function $R_{k_i}^*$ is smaller than $\overline{D_U}(\#P^*)$ by the factor of $c_{k_i}(\#Q)$, i.e. $\Delta(R_{k_i}^*) = c_{k_i}(\#Q) \overline{D_U}(\#P^*)$, where $k_i \leq f_i$. Therefore,

$$\|\Delta(R_i)\|_L = \|\sum_{k_i} c_{k_i}(\#Q) \overline{D_U}(\#P^*)\|_L \leq f_d \|\max_{1 \leq k_i \leq f_i} \{c_{k_i}(\#Q)\}\|_L \overline{D_U}(\#P^*), \quad (6)$$

where $R_i \in S_{OM}$, $f_d = \max\{f_i\}$.

The unfolded sample figure is decomposed into a maximum of f_d compact convex parts/bodies. f_d is called **decomposition degree** and depends on object shape and its unfolding. In this example, $f_d = 39$.

Thus, the discrepancy can be estimated as follows:

$$D(O_M, Q, S_{OM}, L) \leq f_d c(\#Q) \overline{D_U}(\#P^*), \quad (7)$$

where $c(\#Q) \leq 1$ is inversely proportional to the density as well.

Thus, the discrepancy on the surface of the 3D-objects could be compared under the assumptions stated above with the discrepancy of the points distributed on the unit square.

Hence, the discrepancy $D(O_M, Q, S_{OM}, L)$ calculated over the total object mesh depends on the de-

composition degree in the case of small points set; if the point set Q has the cardinality significantly larger than f_d , the decomposition degree f_d does not have a major impact on the discrepancy. Note also, that the discrepancy could be exactly equal to $\overline{D_U}(\#P^*)$ on some local parts of the surface.

Such dependency of discrepancy on size and shape of the test figures containing the respective uniformly distributed point sets is investigated in detail in the next section.

4 ALGORITHMS

In order to minimize the geometric discrepancy over the whole surface, the triangles should be assembled to as large as possible segments while retaining the original neighbourhood of the triangles.

To distinguish between 3D and 2D domains, we denote a (connected) subsection of a triangulated surface as **segment** and its unfolded (flattened) counterpart as **strip**. The effect of discrepancy increase not only applies to edges where segments touch, but everywhere along their edges where their 2D projections are split with a distance smaller than mean distance d_m . A similar effect is caused by the inverse, namely when parts of segments mapped to a strip overlap in a zone up to width d_m . These effects are illustrated in Figure 3. Interstices may likely appear when a polygon mesh representing a curved surface like that of a sphere is flattened; see Figure 2 for an example. The elongated parts of a strip between interstices are denoted as “**fingers**”. If fingers extend over saddle regions in the segment, they may overlap in the strip. In general, the zone of width d_m along the edges of a strip contributes most to the increase of discrepancy, because here the continuity of the point distribution as taken over from unit square U is broken whenever it touches another border.

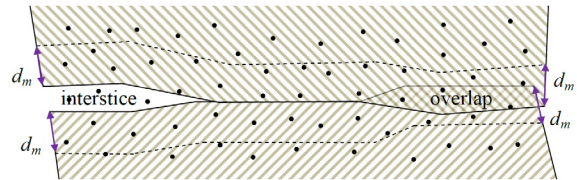


Figure 3: Zones of the strip with larger discrepancy in interstices (left) and overlaps (right). Because the points in overlap regions are mapped to multiple segments, the distances between their copies on the 3D-surface would be smaller than d .

Following these observations, the minimization of the “*irregular border zone*” ΔA can be achieved by following goals:

- Maximize size of segments.
- Minimize ratio edge length / area of strips.
- Minimize elongation of strips.
- Minimize concave zones.
- Minimize number of strips and, therefore, the decomposition degree of the sample figures.
- Planes should not be split.

Optimizing all goals with a single algorithm is difficult if not impossible. This approach will focus on achieving a good balance between these requirements.

4.1 Mesh Segmentation and Unfolding

The simple segmentation-unfolding algorithm we are using works as follows:

- 1) Find the 2D skeleton of the (first) strip:

Starting with the triangle $T_i(e_i(v_i, v_j), e_j(v_j, v_k), e_k(v_k, v_i))$ with the largest edge, e.g. $e_i(v_i, v_j)$, its ordered set of vertices is congruently mapped to the plane. The triangle T_i and vertex v_i are saved in corresponding look-up tables with a mark “is mapped”.

The next triangle T_{i+1} that is chosen is the one attached to the longest of the remaining mapped edges, e.g. v_r , of the previous triangle; and its non-considered vertex is also mapped to the plane, in the same way as vertex v_k . The triangle T_{i+1} and vertex v_r are saved in corresponding look-up tables with mark “is mapped” as well. The process continues until a chosen triangle has already been mapped.

If the longest edge of the start-triangle has a non-mapped adjacent triangle, the process can be pursued in the other direction. When no more triangles can be added to the strip, the ordered sequence of outer edges is saved as *strip-boundary*.

2) In the next step, the algorithm moves along the strip-boundary and adds to the strip those triangles which were not yet added to any strip and which, together with their neighbours from the segment, establish a plane or “almost” a plane, i.e. the minimal angle between them is closed to 180° . By adding the new triangle to the strip, the corresponding boundary edge is replaced by the new edges.

3) Next, we look once more along the boundary to find such leftover triangles that are not yet mapped but are surrounded by unfolded segments.

4) If the cardinality of the strip is smaller than a given threshold, the strip will be allowed to grow again along its boundary, and the steps 2 and 3 will be repeated as long as possible.

5) The accumulation of the next segment and strip starts from the largest edge of the saved strip-boundaries.

The unfolding of the segments onto the plane does not change the area or the geometry of the individual triangles but creates splits and overlapping regions inside or at the border of the strips.

As already mentioned, even tiny gaps can lead to missing sampling points and very small overlapping can cause doubling of points, which both increase the discrepancy. One source of such regions is floating-point operations, because when performed in different orders they do not always lead to exactly the same result. The second one is the roughness of the object surface. In our approach we extract and handle thin interstices and thin overlaps using a correction algorithm (see Section 4.2).

4.2 Low-discrepancy Points Wrapping

The distribution of points on the arbitrary surface is operated in the following manner:

1) The strips generated with the algorithm described before are mapped to a planar domain.

2) Points are scattered on the planar domain that contains the strips. The cardinality of the points set depends of the area of the planar domain and some default density. The default density can be given, for instance, by the user. Because used algorithm generates points in the unit square, the set of points need to be isotropic scaled to the planar domain.

3) The strips are positioned on the planar domain, using another low-discrepancy set of points with cardinality that is equal to the number of strips.

4) The total area of “irregular zones” is calculated for the whole object. If the *irregularity ratio*, i.e. the ratio of the area of “irregular zone” to the total surface area (see Section 4.3), is larger than a given threshold, the used point density is increased (and hence the mean distance d_m between neighbours decreased). All points inside each planar triangle are mapped back to the 3D-surface.

5) The points inside thin interstices and thin overlaps are mapped to the corresponding edges using the following *correction algorithm*:

a) For each strip find thin interstices and thin overlapping regions. A region width of $0.1 d_m$ is used in the examples below;

b) If the interstice contains a point, project it orthogonally onto the closest edge;

c) If the overlapping contains a point, find all corresponding points on the 3-D surface and remove all copies but one.

The next section describes how the accuracy of the approach is estimated by the using of irregularity ratio.

4.3 Unfolding Accuracy

Let R be the irregularity ratio $R=\Delta A/A_{\text{tot}}$, where A_{tot} is the total surface area of the object and ΔA is the area of the “irregular zone”. $\Delta A=\Delta A(b)$ is established along each boundary edge b . Besides d_m , the boundary length and the shape of the strip where b belongs influence $\Delta A(b)$ as well.

The area of the irregular zone can be calculated exactly for simple objects. For complex objects, we establish ΔA for each strip, where the boundary consists of a sequence of ordered edges: $\{e_1, \dots, e_{j-1}, e_j, e_{j+1}, e_{N_e}\}$, where N_e is the number of boundary edges of a strip and edges e_1 and e_{N_e} are neighbours. A rough estimate of ΔA can be calculated as follows:

$$\mathcal{A}(\text{strip}) \leq d_m \sum_{j=1}^{N_e} \text{len}(e_j) + 2 d_m^2 N_{\alpha>\pi}, \quad (8)$$

where $\text{len}(e_j)$ is the length of the edge e_j and $N_{\alpha>\pi}$ is a number of concave strip vertices.

To calculate a more precise estimation of value for ΔA , the following cases could be considered:

- a) the “irregular zone” adjacent to e_j is a triangle;
- b) the “irregular zone” adjacent to e_j is a rectangle, avoid in this case that some areas do not calculated twice;
- c) at least one of the half-angle between the edges adjacent to e_j is larger than 90° , the corresponding corner of the “irregular” trapezoid or parallelogram could be reduced to a circular sector.

The whole value of ΔA is accumulated along the boundary of the strip. Note, that the irregular area within thin “fingers” or zones with a width $< 2 d_m$ could be calculated twice. In our approach we do not search for such overlaps but use them to weight the irregularity ratio if the strip has unwanted thin “fingers” or zones. Therefore, in some cases the ratio R can be larger than 1.

An important concept in computer graphics is that of *level-of-detail* (LoD): a prescribed resolution depending on the distance between camera and the object (more precisely, some fixed point of the object, e.g. its centre). Evidently, calculated points set with large R can be effectively used at large LoD to estimate the visible surface fraction. In general, the balance between the irregularity ratio and density should be deciding for each LoD.

5 EXPERIMENTAL RESULTS AND DISCUSSION

The low-discrepancy points wrapping approach is tested by using the different surface meshes, including meshes of geometrically simple objects (Figure 4), analytically calculated meshes (Figure 5), and meshes which are produced by a laser scanner with adaptive re-meshing (Figure 7) and without re-meshing (Figure 6). Such meshes do not only differ in topology and in the number of connected components, but some of them are also not optimized to achieve a regular and/or structured grid.

Figure 4 shows the scattering of points onto a sphere. The mesh has a structured curvilinear grid. The segmentation algorithm yields one segment, of which the two-dimensional projection (Figure 4e) has many tiny interstices. The points provided by the correction algorithm are shown in Figure 4f in pink colour. To achieve the irregularity ratio of 0.95, 770 points shall be scattered, while the distribution of the 192 points leads only to irregularity of $R=1.32$.

By using the Hammersley algorithm in the spherical coordinates (Wong et al., 1997) we can also calculate the low-discrepancy points set distributed directly onto the spherical surface and compare them with our approach, see Figures 4a and 4b versus 4c and 4d, respectively.

In the next example the low-discrepancy points wrapping approach is applied to an object created analytically by a cup-generator, the object is shown in Figure 5. The mesh has a block structured grid, but, in general, is not regular. The planar strips have a lot of gaps and overlapping regions because of the smoothed surface and non-trivial geometry. The algorithm distributes 550 points with irregularity $R=0.3$. Figures 5b, 5c and 5d show the obtained points from different point of view.

The approach is also tested for some natural objects, which were produced using a laser scanner. One of them, “Fruit Drink” we can see in Figure 6 (see also www.iaim.ira.uka.de/ObjectModel/). The original object surfaces are not perfectly smoothed and have a lot of knock, wrinkles and bowings. The meshes have not been optimized and have, therefore, unstructured grid arrangements. The mesh is automatically segmented in 32 segments, which cuts are given in Figure 6a in different colours. The largest strip with 21963 triangles is shown in Figure 6b. (The remaining 31 segments together contain no more than 3031 triangles.) The Figures 6c and 6d illustrate the distribution of 56 and 315 sample points, respectively, onto object surface with irregularity rate $R=1.07$ and $R=0.22$, respectively. In Fig-

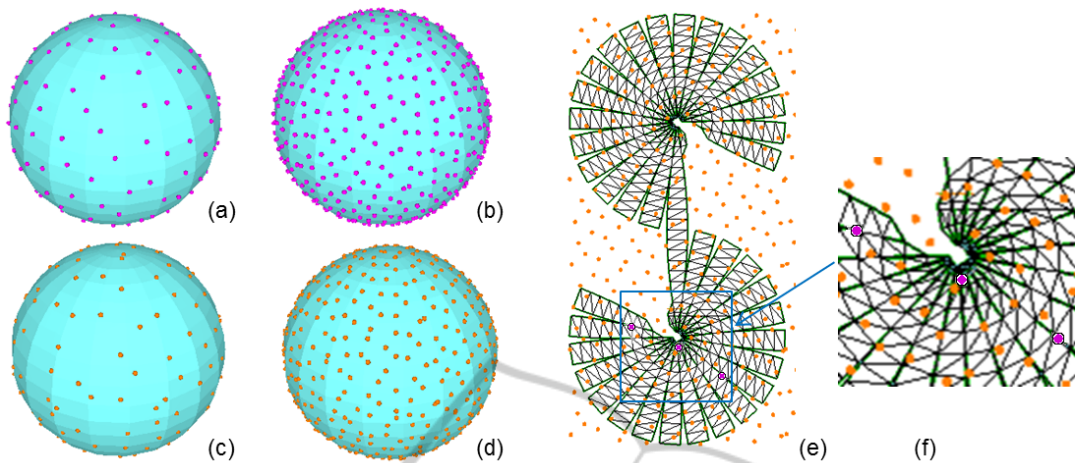


Figure 4: Sphere: #vertices =382; #edges=1140; #triangles=760; #strips=1; Hammersley algorithm in the spherical coordinates: (a) #points=192, (b) #points=770; low-discrepancy points wrapping approach: (c) #points=192, $R=1.32$; (d) #points=770, $R=0.95$; (e) 2D strip; (f) image enlargement.

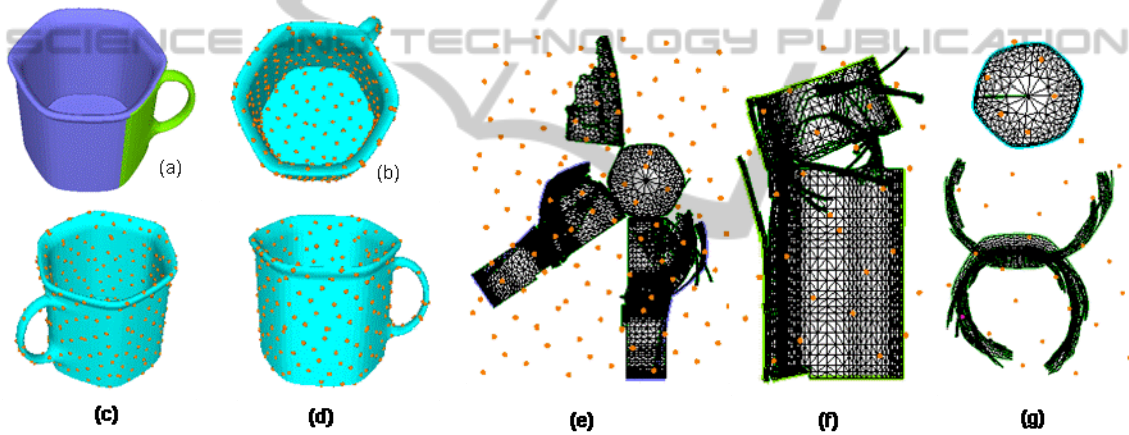


Figure 5: Cup: #vertices =7024, #edges =20976, #triangles =13952, #strips=4; (a) segmentation; (b), (c) and (d) different views of #points=550, $R=0.30$; (e), (f) and (g) 2D strips with #points=65 and $R=1.73$.

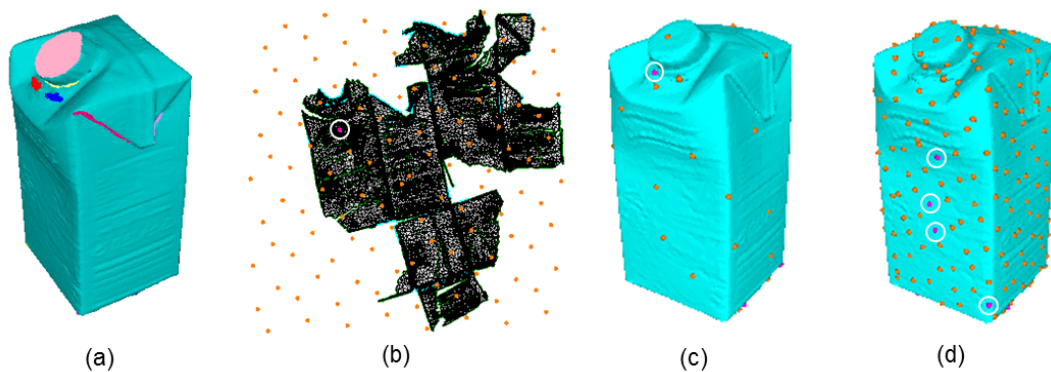


Figure 6: Fruit Drink: #vertices =12487, #edges =37495, #triangles =24994, #strips=32; (a) segmentation; (b) the largest strip with 21963 triangles; (c) #points=56, $R=1.07$; (d) #points=315, $R=0.22$.

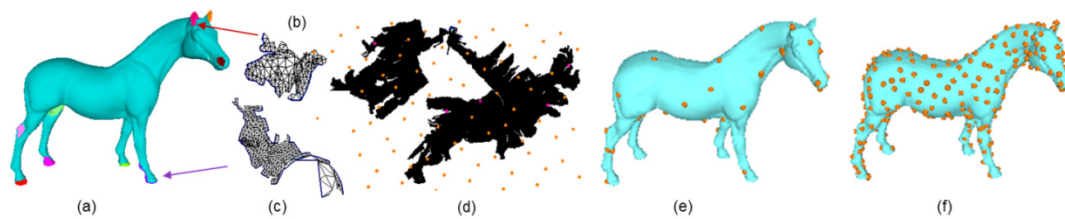


Figure 7: Horse: #vertices=48485, #edges=145449, #triangles=96966, #strips=28; (a) segmentation; (b) and (c) small 2D strips with 252 and 520 triangles, respectively, (d) the largest 2D strips with 93754 triangles; (e) $R=1.65$, #points=57; (f) $R=0.25$, #points=335.

ure 6b we also can see the pink points added by the correction algorithm.

The last example in Figure 7 demonstrates the application of our approach to a large model (see http://www.cc.gatech.edu/projects/large_models/horse.html), whose mesh is produced by laser scanner and has an unstructured grid, but it is well smoothed. The mesh is cut into 28 segments. The mapping of the largest one to the plane is shown in Figure 7d and two smaller strips are given in Figure 7b and 7c. The distribution of 335 points occurs with irregularity ratio $R=0.25$ and 28 sample points are scattered with $R=1.65$.

6 CONCLUSIONS

In this work, we describe an approach for low-discrepancy distribution of sample points on triangulated surfaces of arbitrary 3D objects within a wide density range. The accuracy of the performed technique is determined by the ratio between the area of the irregular zone and the total area. A wide range of possible point densities can be used to conform to different level-of-details.

Our intent was to distribute as few points as possible on a 3D-surface so that from each view a sufficient number of points is visible, which corresponds to the visible fraction of the surface (with respect to the required LoD). Examples indicate that good results can already be achieved with less than 100 points, which is clearly smaller than the numbers usually reported in literature (see Section 2).

An important question is how to perform the segmentation and the unfolding in a way which minimizes the raise in the discrepancy. The further research will focus, therefore, on the mesh segmentation and the unfolding as an optimisation problem.

Additional work will address the direct measurement of the resulting geometric discrepancy on the surface itself.

REFERENCES

- Alexander, J. R., Beck, J., Chen, W. L., 2004. Geometric discrepancy theory and uniform distribution. In *Handbook of Discrete and Computational Geometry*, Boca Raton: Chapman & Hall/CRC, 2nd Edition.
- Berg, M., 1996. Computing half-plane and strip discrepancy of planar point sets. *Comput. Geom.* 6: 69-83.
- Chen, W. W. L., Travaglini, G., 2007. Discrepancy with respect to convex polygons. *J. Complexity.* 23(4-6):662-672.
- Cheng, J., Druzdzel, M. J., 2000. Computational investigation of low-discrepancy sequences in simulation algorithms for Bayesian networks. In *Proceedings of the 16th Conference on Uncertainty in Artificial Intelligence*. pp. 72-81.
- Cui, J., Freedman, W., 1997. Equidistribution on the sphere. *SIAM J. Sci. Comput.* 18(2):595-609.
- Dachsbacher, C., Stamminger, M., 2006. Splatting indirect illumination. In *Proceedings of the 2006 symposium on Interactive 3D graphics and games (I3D '06)*. pp. 93-100.
- Grabner, P.J., Hellekalek, P., Liardet, P., 2012. The dynamical point of view of low-discrepancy sequences. *Uniform Distribution Theory.* 7(1):11-70.
- Halton, J. H., 1960. On the efficiency of certain quasi-random sequences of points in evaluating multi-dimensional integrals. *Numer. Math.* 2:84-90.
- Hammersley, J. M., 1960. Monte Carlo methods for solving multivariable problems. *Ann. New York Acad. Sci.* 86:844-874.
- Hanson, K. M., 2003. Quasi-Monte Carlo: half-toning in high dimensions?. In *Proceedings SPIE 5016*. pp.161-172.
- Hofer, R., Pirsic, G., 2011. An explicit construction of finite-row digital $(0,s)$ -sequences. *Uniform Distribution Theory.* 6:13-33.
- Matousek, J, 1999. *Geometric Discrepancy – An Illustrated Guide*. Algorithms and combinatorics series, Vol.18; Springer, Berlin Heidelberg.
- Niederreiter, H., Chao, X, 1995. Low-discrepancy sequences obtained from algebraic function fields over finite fields. *Acta Arithmetica*, 72:281-298.
- Pillards, T., Cools, R., 2005. Transforming low-discrepancy sequences from a cube to a simplex. *J. Comput. Appl. Math.* 174(1): 29-42.

- Quinn, J. A., Langbein, F. C., Martin, R. R., 2007. Low-discrepancy point sampling of meshes for rendering. In: *Symp. on Point-Based Graphics 2007*. pp. 19-28.
- Rakhmanov, E.A., Saff, E.B., Zhou, Y.M., 1994. Minimal discrete energy on the sphere. *Math. Res. Lett.* 1:647-662.
- Rovira, J., Wonka, P., Castro, F., Sbert, M., 2005. Point sampling with uniformly distributed lines. *Eurographics Symp. Point-Based Graphics*. pp. 109-118.
- Shamir A., 2008. A Survey on Mesh Segmentation Techniques. *Computer Graphics Forum*. 27(6): 1539-1556.
- Sobol, I. M., 1967. On the distribution of points in a cube and the approximate evaluation of integrals. *U.S.S.R. Computational Mathematics and Mathematical Physics*, 7(4):86-112.
- Wand, M., Straßer, W., 2003. Multi-resolution point-sample raytracing. In: *Graphics Interface 2003 Conference Proceedings*.
- Wong, T.-T., Luk, W.-S., Heng, P.-A., 1997. Sampling with Hammersley and Halton points. *Journal of Graphics Tools*. 2(2):9-24.

